Journal of Agricultural Sciences (JAS) 32(4):967-987
DOI: 10.15832/ankutbd.1868589

J Agr Sci-Tarim Bili
e-ISSN: 2148-9297
jas.ankara.edu.tr

Development of Irrigation Automation System Based on FAO Penman-Monteith Model with Drip Irrigation for Paddy Rice

Hakkı Fırat Altinbilek[a*], Ünal Kizil[b], Gökhan Çamoğlu[b], Sefa Aksu[b], Hakan Nar[b]

[a]*Ministry of Agriculture and Forestry, Bayramiç District Directorate, 17700, Bayramiç, Çanakkale, TÜRKIYE*

[b]*Çanakkale Onsekiz Mart University, Department of Agricultural Structures and Irrigation, Faculty of Agriculture, 17020, Çanakkale, TÜRKIYE*

ARTICLE INFO
Research Article
Corresponding Author: Hakkı Fırat Altinbilek, E-mail: hfirataltinbilek@gmail.com
Received: 21 January 2026 / Revised: 04 May 2026 / Accepted: 06 May 2026 / Online: 12 October 2026

Cite this article
Altinbilek H F, Kizil Ü, Çamoğlu, Aksu S, Nar H (2026). Development of Irrigation Automation System Based on FAO Penman-Monteith Model with Drip Irrigation for Paddy Rice. *Journal of Agricultural Sciences (Tarim Bilimleri Dergisi),* 32(4):967-987. DOI: 10.15832/ankutbd.1868589

ABSTRACT
The increasing demand on water due to drought impacts paddy rice production. Therefore, the use of sustainable irrigation methods and smart agricultural practices are of gaining importance. In this study, it was aimed to provide drip irrigation automation by calculating paddy rice evapotranspiration (ET_C), irrigation water requirement and irrigation duration based on FAO Penman-Monteith (FAO-PM) model with the developed prototype device via mobile application. Four different irrigation levels (S100, S150, S200 and Farmer (F)) were applied in the study. The research was carried out in the farmer's field located in İpsala district of Edirne province in 2023 and 2024 seasons. The trial was carried out based on daily meteorological parameters in field conditions and the data were stored in a Sheets file on Google Drive. In the study, the seasonal total reference evapotranspiration (ET_0) and ET_C values were calculated as 571 and 583 mm in 2023 and 655 and 665 mm in 2024. Ranges of seasonal total irrigation water applied were 695-1555 mm in 2023 and 802-1916 mm in 2024. In 2023, the highest yield was obtained in the F application at 6502 kg/ha, while the lowest yield was obtained in the S100 application at 4552 kg/ha. In the second year of the study, the highest yield was obtained in the F application at 7401 kg/ha, while the lowest yield was obtained in the S100 application at 5381 kg/ha. In the first year of the study, irrigation water use efficiencies (IWUE) varied between 0.42-0.65 kg/m^3 and between 0.39-0.67 kg/m^3 in the second year. The highest IWUE was found in the S100 application in both years. As a result of the study, it was revealed that the system successfully performed irrigation automation. It was seen that the developed device was also applicable for small businesses in terms of ease of use.

Keywords: Automation, Crop water requirement, Irrigation scheduling, Real-time monitoring

1. Introduction

Rice (*Oryza sativa L.)* is among the most important cereal crops globally, supplying more than 20% of the world's caloric intake and serving as the primary food for over 3.5 billion people (Hashim et al. 2024). The cultivation of rice is concentrated predominantly in Asia, which accounts for nearly 90% of global production. Major producing countries such as China, India, Indonesia, and Bangladesh together represent a significant portion of total production (Glauber & Mamun 2024; Darko et al. 2025). In comparison, Türkiye accounts for a modest share of global paddy rice production of approximately 900,000 tons. Nonetheless, rice remains a strategically important crop in the country, largely fulfilling domestic demand and playing a critical role in regional agricultural economies, particularly in provinces like Edirne, Samsun, Balıkesir & Çanakkale (Çığ et al. 2024; Gaytancıoğlu & Yılmaz 2024; TÜİK 2025).

Paddy rice cultivation is characterized by exceptionally high water demand, primarily due to the widespread use of continuous flooding irrigation practices. Under this traditional management approach, a shallow water layer is maintained on the soil surface throughout most of the vegetative growth stage of the crop. While continuous flooding is effective in suppressing weed competition and moderating soil temperature, it is inherently inefficient in terms of water use (Amin et al. 2021). Globally, rice irrigation is estimated to consume 30–45% of total freshwater allocated to agriculture (Surendran et al. 2021). This high-water demand poses serious challenges in the context of diminishing freshwater resources, increasing competition for water between agricultural and urban sectors, and the accelerating impacts of climate change (Li et al. 2020; Yazdanpanah et al. 2022).

In recent decades, climate change has increased hydrological uncertainty by altering precipitation regimes, intensifying drought events, and increasing ET_C (Dai et al. 2018; Qiu et al. 2023). These shifts necessitate a transition toward water-saving irrigation technologies that enhance efficiency without compromising productivity. Among the various alternatives proposed, drip irrigation has emerged as a promising solution for paddy systems (Sharda et al. 2017; Nabipour et al. 2024). It improves irrigation

water use efficiency (IWUE), fertilizer uptake and, in some cases, yield stability under water-limited conditions (Parthasarathi et al. 2018; Demirel et al. 2020; Samoy-Pascual et al. 2022).

The adoption of drip irrigation systems, however, demands precise and site-specific management. Unlike flood systems, drip irrigation does not provide a buffer against under- or over-irrigation; therefore, accurate scheduling based on ET_C is essential. Among the various empirical and semi-empirical models available, the Penman-Monteith equation, standardized by the FAO as the reference method (FAO-56), remains the most robust and scientifically accepted model due to its strong physical foundation and adaptability to various climatic conditions (Allen et al. 1998; Irmak et al. 2003; Er-Raki et al. 2007; Córdova et al. 2015; Celestin et al. 2020; Islam & Alam 2021; Dai et al. 2022).

The FAO-PM method requires accurate input data, including air temperature, relative humidity, solar radiation, and wind velocity, to compute daily ET_0. Numerous studies have validated the model's performance across a wide range of agroclimatic zones and cropping systems (Cai et al. 2007; Lang et al. 2017; Köksal et al. 2022; Tunca & Köksal 2024). However, the practical application of the FAO-PM model in small farming systems is often limited by the unavailability of continuous, high-quality meteorological data, particularly in remote or resource-constrained areas. This data gap represents a major barrier to the implementation of scientifically designed irrigation scheduling practices at the field level (Sentelhas et al. 2010; Moratiel et al. 2020).

Recent advances in sensor technology, embedded electronics, wireless communication, and open-source microcontroller platforms have opened new possibilities for the development of affordable environmental monitoring and control systems. In particular, the Arduino ecosystem has gained widespread popularity in precision agriculture applications due to its low cost, modularity, and ease of integration with various environmental sensors (Gündoğdu et al. 2020; Kızıl et al. 2022; Pearce et al. 2024; Yıldırım et al. 2025). These systems allow for real-time data acquisition, local processing, wireless data transmission, and automated control of irrigation valves and pumps, thereby enabling the implementation of smart irrigation systems even in low-resource settings (Aksu & Kızıl 2020; Kondaveeti et al. 2021; Ogidan et al. 2023). Moreover, the integration of such systems with remote access interfaces via mobile applications or cloud-based platforms enhances user interaction, allowing for greater flexibility, decision-making support, and system responsiveness. The ability to dynamically adjust irrigation based on real-time meteorological and crop-specific data represents a significant step toward climate-smart agriculture and the broader goals of sustainability, productivity, and resilience (Kondaveeti et al. 2021; Kulmány et al. 2022; Pearce et al. 2024).

The aim of this study is to design and develop a cost-effective, user-friendly smart irrigation automation system specifically tailored for small scale paddy rice operations. The system utilizes real-time meteorological data obtained from a low-cost mini weather station and integrates the FAO-PM method to compute daily ET0 and ETC requirements. The calculated irrigation demands are then used to automate a drip irrigation system, with additional capabilities for mobile-based remote monitoring and control. By merging scientific irrigation modeling with accessible digital tools, this study addresses the critical need for scalable and affordable irrigation solutions in water-stressed agricultural regions and contributes to the ongoing transition toward data-driven, sustainable rice production systems.

2. Material and Methods

2.1. Study area and experimental design

The study was conducted in a farmer's rice field located at 40.8865 °N latitude and 26.3712 °E longitude in İpsala (Figure 1), a district of Edirne province, which alone accounts for 19% of Türkiye's total paddy rice production. The research was carried out during the 2023 and 2024 growing seasons. The experimental site was characterized by a heavy clay soil, with a clay content of approximately 63.8%, indicative of a very fine-textured profile. The soil exhibited a relatively low infiltration rate was around 7.3 mm/h. In the upper 0–30 cm layer of the soil profile, the measured properties were as follows: organic carbon content was 1.51%, soil pH was 7.34, lime content was 0.22%, electrical conductivity (EC) was 1.35 mS/cm, and total nitrogen content was 0.08%.

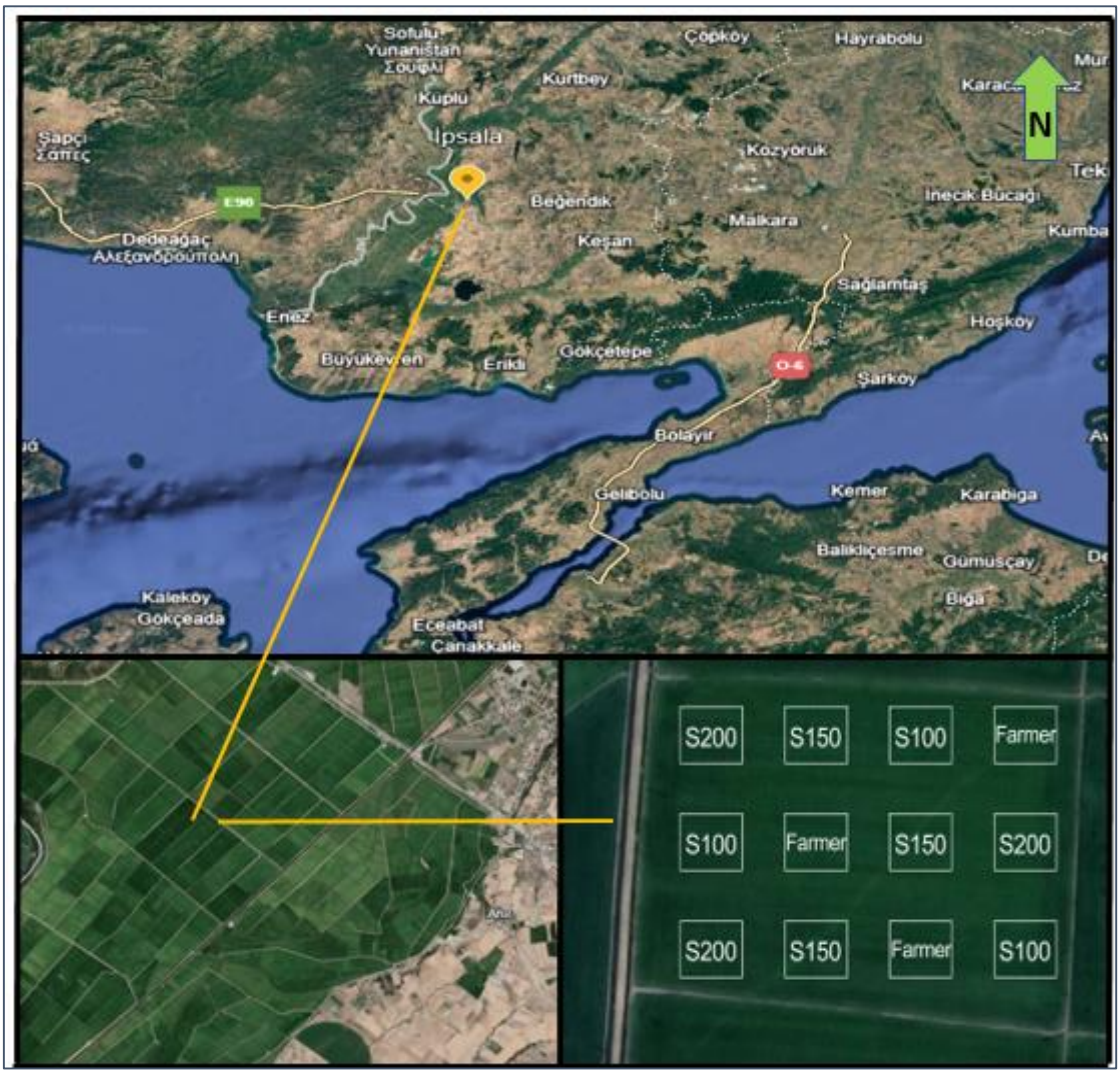


Figure 1 - Study area

The drip irrigation system used in the trial consists of solenoid valves, ball valves, water meters, in-line drippers, irrigation pipes, control unit and pump. The irrigation system consists of a main pipeline with a diameter of 40 mm and a manifold pipeline with a diameter of 32 mm. The dimensions of the wetting area were analyzed, and the most appropriate flow rate and intervals of the drippers were selected. The laterals in the system were 16 mm in diameter and contain on-line pressure regulated drippers placed at 50 cm intervals. The flow rates of these drippers were 4 L/h. The experiment was conducted using a randomized block design with four irrigation treatments and three replications. The widely cultivated and regionally adapted rice (*Oryza sativa L.*) cultivar Keşhan was used as the plant material due to its high yield potential and suitability for local agro-climatic conditions. The individual plots were arranged in dimensions of 5 m × 5 m. To prevent interaction between adjacent plots, 5 m buffer zone was left around each plot (Figure 2).

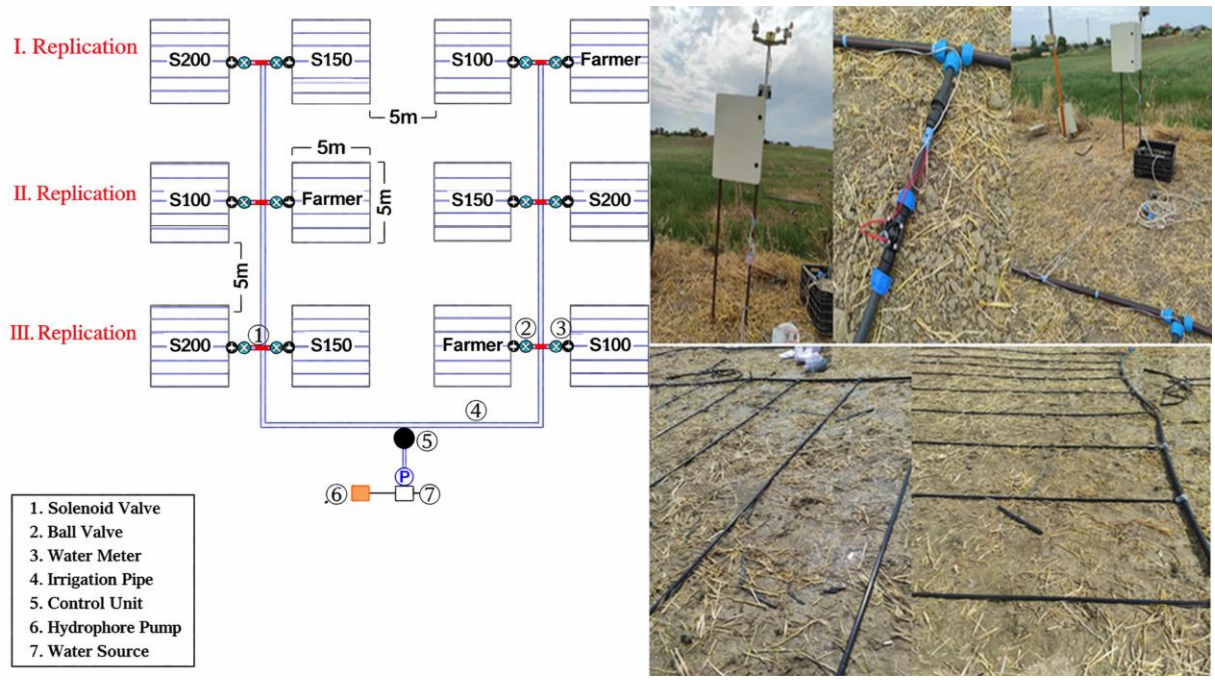


Figure 2 - Experiment design

Prior to the experiment, the physical properties of the soil were determined (Table 1). Soil profiles were excavated at three representative locations within the experimental field, and samples were collected from each of the 0–30 cm, 30–60 cm, 60–90 cm, and 90–120 cm soil layers. The collected samples were analyzed for field capacity, permanent wilting point, bulk density, and soil textural class, following the procedures outlined by Tüzüner (1990). Field capacity and permanent wilting point were determined using a pressure plate apparatus at 1/3 atm and 15 atm, respectively.

Table 1 - Soil characteristics

Depth (cm)	*Soil Textural Class*	*Bulk Density (g/cm^3)*	*Field Capacity (%)*	*Permanent Wilting Point (%)*
0-30	Clay-loam	1.31	30.36	20.58
30-60	Clay-loam	1.33	30.64	20.93
60-90	Clay-loam	1.34	30.28	19.61
90-120	Clay-loam	1.36	29.87	19.82

The irrigation treatments evaluated in the experiment are presented in Table 2. Irrigation treatments were systematically defined as proportional levels of crop water requirement derived from ET_0 estimates. The S100 treatment was designed to represent full irrigation, in which the entire calculated ET_C demand was replenished at each irrigation event to avoid water stress. In contrast, S150 and S200 treatments correspond to over irrigation scenarios, where 150% and 200% of ET_C were applied, respectively, to evaluate the robustness and adaptive response of the developed irrigation system under excessive water supply conditions and to simulate potential mismanagement or conservative farmer behavior. F treatment was implemented based on conventional irrigation habits in the region, typically characterized by fixed-interval irrigation without quantitative assessment of crop water requirements, thereby serving as a benchmark for comparison with the automated ET_C-based approach.

Irrigation in the S100, S150, and S200 plots was carried out during the early morning hours between 07:00 and 09:00, when the ET_C was at its lowest. For the farmer-managed irrigation treatment, the same irrigation duration used by the farmer was taken into account.

Table 2 - Irrigation treatments

Treatment	
S100	100% of real-time calculated of ET_C
S150	120% of real-time calculated of ET_C
S200	200% of real-time calculated of ET_C
Farmer (F)	Application of the farmer's own irrigation strategy

2.2. Electronic components

Daily values of temperature (T), atmospheric pressure (P), sunshine duration (n), wind velocity at 2 meters (U_2), and relative humidity (RH) were obtained using sensors. In addition to these parameters, daily total precipitation was measured by a pluviometer connected to the system. An Arduino-compatible station containing the sensors required to measure these parameters was installed in the field. For this purpose, a mini meteorological station ADS-WS1 (Argent Data Systems, Santa Maria, California, USA) was used. The station is equipped with a wind vane, an anemometer, and the corresponding mounting accessories for the sensors. The driver board, to which the sensors are connected via RJ11-type connectors, can acquire temperature and humidity data through the integrated AM2320 sensor (Aosong Electronics Co. Ltd., Huangpu, Guangzhou, China) embedded on the board. In addition, the driver board is equipped with a BMP280 barometric pressure sensor (Bosch Sensortec GmbH, Tübingen, Baden-Württemberg, Germany). The rain gauge integrated into the ADS-WS1 weather station is a tipping-bucket type pluviometer designed for automated precipitation measurement. It records rainfall depth (mm) with a typical resolution of 0.2 mm per tip and operates with low power consumption and high measurement stability.

The designed system initially requires caching of sensor data. For this purpose, the data acquisition module of the meteorological station was employed. Passive sensors such as the anemometer and pluviometer, which are physically connected to the module, provide time-dependent pulse counts corresponding to wind movement and precipitation, respectively. Subsequently, the data acquisition board computes the actual wind velocity and precipitation amount using calibration equations specific to each sensor. In contrast, the temperature-humidity and atmospheric pressure sensors attached to the data acquisition board are digital sensors capable of generating real-time measurements. However, these sensors cannot simultaneously transmit data at the same time interval due to differences in their operating protocols. To ensure that all sensor data are collected concurrently, an Arduino Mega development board based on the ATmega2560 microcontroller was utilized. The sensor data transmitted from the data acquisition module to the development board via serial communication (Tx-Rx) were cached to enable the calculation of time-dependent averages. Additionally, the total duration of sunshine over a 24-hour period was recorded in the cache using an LDR (light-dependent resistor) sensor connected to the analog terminals of the development board. A parabolic Fresnel lens was employed to focus sunlight, arriving at varying angles throughout the day, onto the LDR sensor. This lens also served as a protective enclosure to shield the LDR from moisture and precipitation. Since the data generation intervals of the sensors used in the system vary from one another, it was necessary to assign a timestamp to each individual data point. For this purpose, a digital real-time clock (RTC) module was integrated into the development board. To transmit the calculated average and cumulative sensor values to an Android device, an HC-05 Bluetooth module (ITEAD Intelligent Systems Co. Ltd., China) was utilized. This module was selected due to its capability to support bidirectional wireless data communication. In order for the system to function properly, an Android-based smart device was positioned in close proximity to the sensor unit. Irrigation operations were carried out via commands sent over the Bluetooth connection to a relay board, which was connected to solenoid valves. The components used in the prototype device and their interconnections are illustrated in Figure 3.

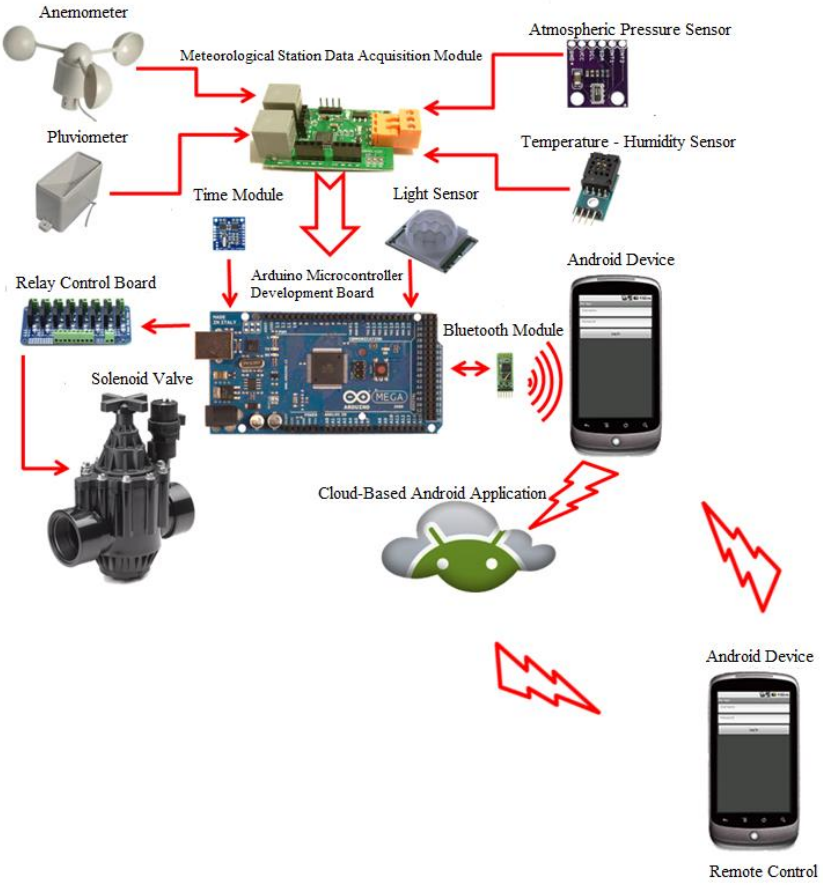


Figure 3 - Components of the prototype device

Sensor data from six different environmental parameters were continuously recorded in the cache memory of a microcontroller development board over a 24-hour period. At the end of each day, embedded software computed cumulative values (for precipitation), average values (for wind velocity, atmospheric pressure, temperature, and humidity), and total daylight duration. These values were transmitted to an Android-based smart device, which also provided geolocation and date information. Based on this combined dataset, ET_0, ETc and the required water amount were calculated at 23:59. All relevant daily data, including sensor readings, FAO-PM model parameters, and the calculated irrigation water requirement, were automatically uploaded at 23:59 to a cloud-based spreadsheet application hosted on Google Drive via the Android device's mobile internet connection. The irrigation volume for the following day was determined based on these values recorded the previous night. Irrigation operations were carried out through commands sent via Bluetooth to a relay board connected to solenoid valves. The system's hourly water delivery capacity was calculated based on the total emitter discharge rates of the drip irrigation network. Using this, the duration for which the solenoid valve should remain active was programmed within the custom-developed Android application. Once the required volume of water was delivered, the system shut down automatically. To initiate irrigation at the scheduled time, pressing the "Start Irrigation" button within the application was sufficient. However, considering scenarios in which on-site access was not possible, a remote access protocol was integrated into the Android application. This allowed irrigation to be triggered via SMS messages from remote mobile devices. For example, sending an SMS with the message "Start1" to the Android device placed near the sensor module would initiate irrigation, while sending "Stop1" would terminate it. To prevent unauthorized control, the application was programmed to ignore SMS messages from unrecognized phone numbers, thereby restricting remote access to only designated users. One of the key reasons for utilizing the Google Sheets cloud-based platform was to establish a centralized database and avoid excessive use of the local storage on the Android device. Another significant advantage was the ability to remotely monitor the sensor data integrity and system performance from any internet-connected computer or mobile device before initiating irrigation. Thus, the performance of sensors and other system components could be observed in real time. In the event of temporary internet unavailability, the Android device stored the calculated values for the past week in its internal memory. This local backup ensured that irrigation could still be triggered via Bluetooth even if cloud access was interrupted at the scheduled irrigation time. The application continuously monitored the internet connection and automatically synchronized data with Google Sheets as soon as connectivity was restored. The operational flow of the entire system is illustrated in Figure 4.

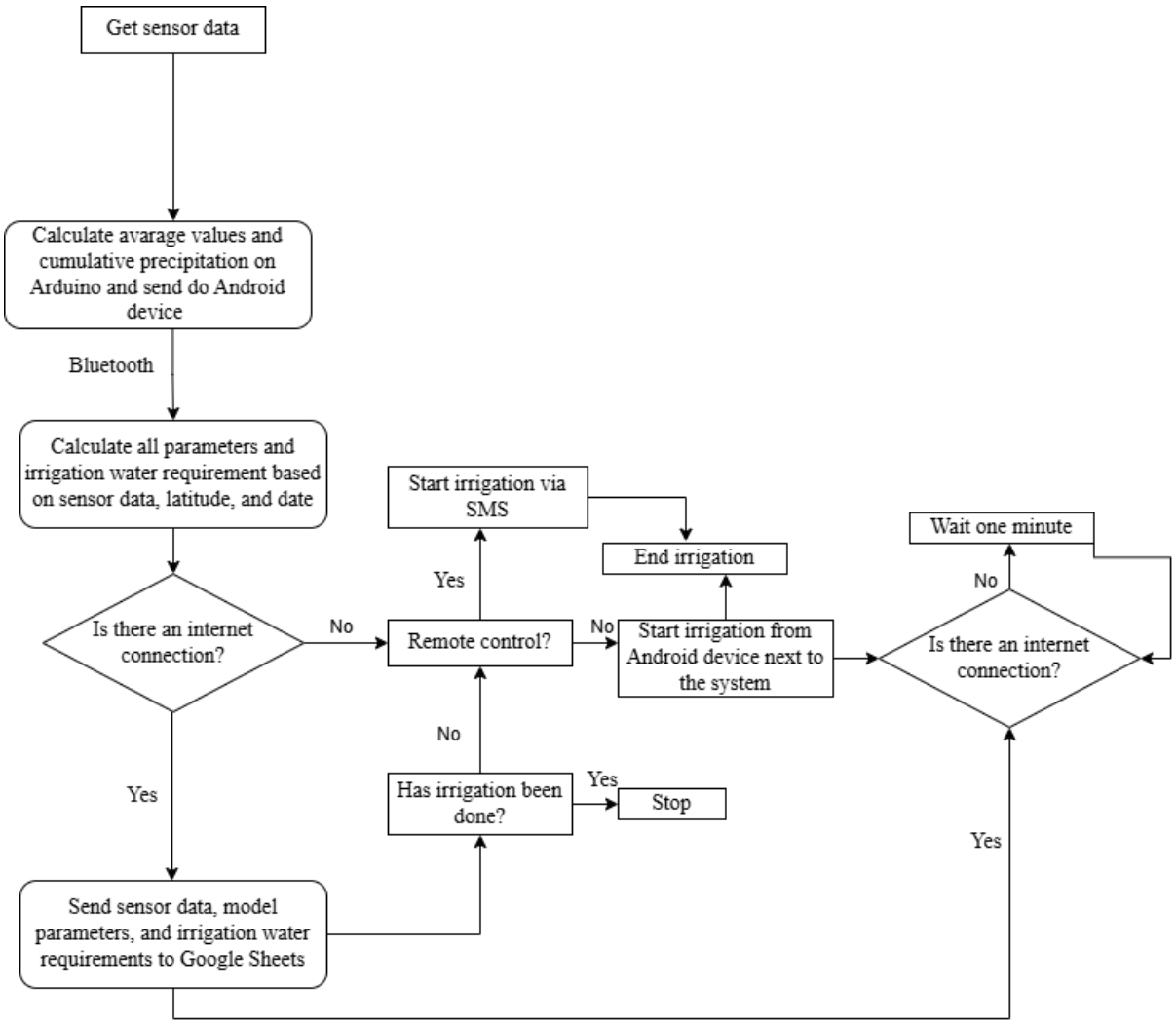


Figure 4 - Flowchart of the irrigation automation system

In the Arduino, sensor input-output pins and libraries were first defined. Sensor data transmissions were performed with the serial communication protocol included in the loop function. Separate reading mathematical command operations were applied to regulate sensor values independently of each other. The average of hourly measured values for temperature, relative humidity and atmospheric pressure was taken from the sensor data transferred to the Arduino Mega in the developed software. The anemometer connected to the system gives 5-minute average wind velocities. The daily averages of these 5-minute average wind velocities were taken to calculate the average wind velocity value at 2 meters. In the calculation of the daily observed sunshine duration (n), the value given by the light sensor at the moment of transition from darkness to light in the laboratory environment was taken as the threshold. When this threshold value was reached, the value given by the sensor was accepted as the value at which illumination began, and the daytime sunshine duration was taken into account as the time between the morning and evening when this threshold value was reached. The pluviometer automatically gives the daily total precipitation without any calibration or processing.

The data obtained in this way and processed on the Arduino Mega microprocessor card and made ready for use was sent to the application on the Android-based device via the Bluetooth module. From this point on, all operations were performed on the Android device. The MIT App Inventor 2 application development platform was used in the preparation of the application developed for the Android device.

While the proposed system demonstrated reliable performance under experimental conditions, specific measures were implemented to enhance its long-term durability and operational stability under field environments. To mitigate the susceptibility of sensors to environmental stressors such as temperature fluctuations, humidity, and dust, all sensing units were enclosed within protective housings and operated under recommended conditions. In addition, periodic calibration procedures were incorporated into the system protocol to minimize sensor drift and maintain measurement accuracy over time. System reliability was further enhanced by ensuring a stable power supply and communication infrastructure; in this context, a backup generator system was integrated to provide uninterrupted energy and to minimize potential interruptions in data acquisition and irrigation control. Although irrigation scheduling may be influenced by spatial variability and extreme climatic conditions, the system was designed

to utilize site-specific meteorological measurements, thereby improving its representativeness for field conditions. These precautions collectively increased the robustness of the system.

2.3. Mobile application

The mobile application, developed for Android devices, was created using MIT App Inventor 2, a free application development tool that allows sensor and Bluetooth connections to be made without requiring coding. In the proposed application, the initial step involves entering field-related information, including location data, field size, and emitter specifications. Following the establishment of Bluetooth communication between the Android device and the Arduino processor, the parameters corresponding to all sensor readings are displayed on the mobile application interface. Subsequently, ET_C is calculated for each treatment using the FAO-PM model, and the required irrigation duration is determined accordingly. Based on these calculations, the system was automatically operated for each replication in line with the prescribed irrigation time. For the F treatment, the amount of irrigation water applied via the drip irrigation method on the adjacent producer's field was taken as a reference. In this case, a sensor attached to the pump used by the farmer enabled the application to calculate the required irrigation duration in the background of the interface according to the volume of water applied, thereby ensuring that the F treatment was irrigated under comparable conditions (Figure 5).

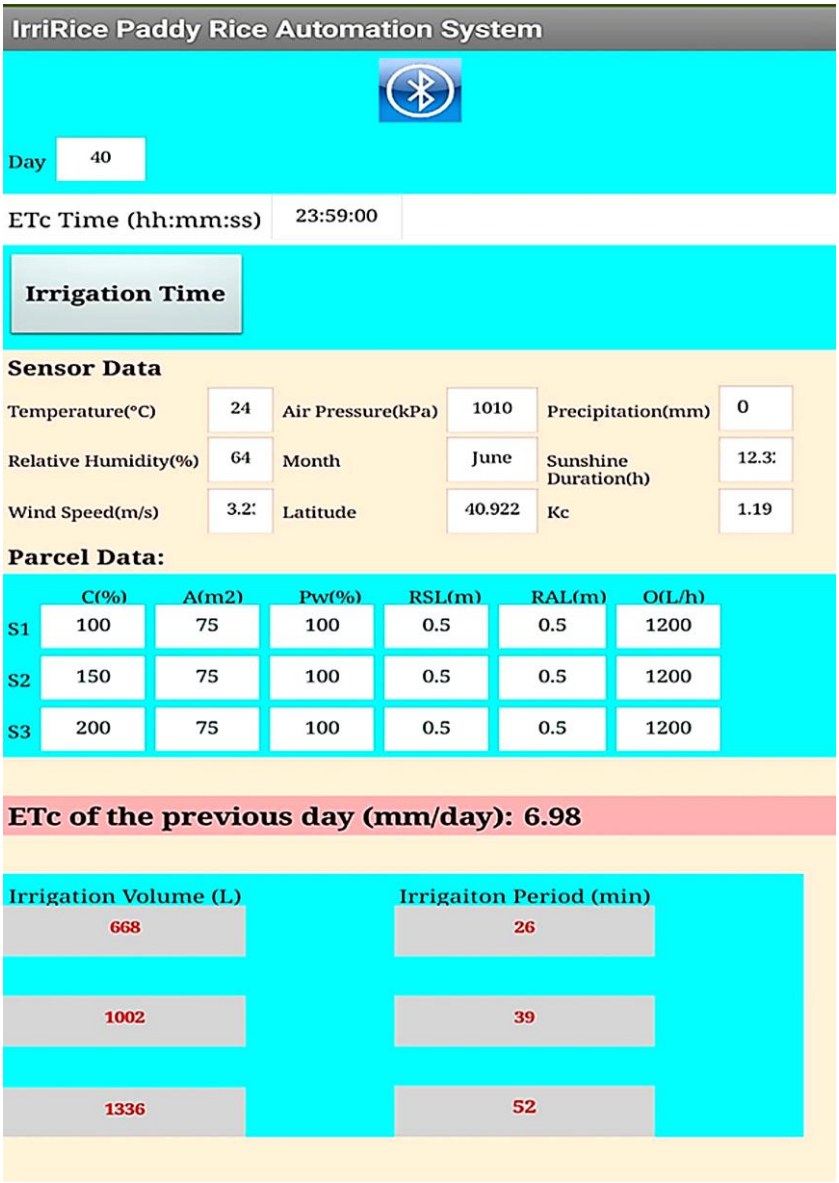


Figure 5 - Mobile application

2.4. Database

Sensor data received and processed via Bluetooth by the smartphone was stored in a spreadsheet file on Google Drive through internet connectivity. For this process, it is sufficient for the smart device to be connected to the internet. The data is transmitted

to the Google Spreadsheet after each reading and systematically recorded there. As a cloud-based data management platform, Google Sheets requires a designated URL endpoint to receive and store incoming data. To instruct the platform on how to interpret and handle these incoming data streams, a series of custom scripts were developed. These coding operations were executed using the Google Apps Script environment, which is accessible directly through Google Drive.

The data stored in Google Sheets is a set of parameters including location, date, time, temperature (°C), relative humidity (%), air pressure (hPa), wind velocity (m/s), sunshine duration (h), precipitation (mm), ET_0 (mm), ET_C (mm), irrigation water amount 1 (L), irrigation water amount 2 (L), irrigation water amount 3 (L), irrigation duration 1 (h), irrigation duration 2 (h), and irrigation duration 3 (h).

Up to this point, the coding and URL configurations were designed to establish communication between the script file and the Google Spreadsheet within the cloud-based system. The interaction between the device and the cloud system was carried out through the URL of the script file. This script URL was embedded into the Android application during its development phase, specifying the exact web address to which the processed data should be transmitted. In this way, an online database structure was created for real-time data storage and access (Figure 6).

SulamaData

Dosya Düzenle Görünüm Ekle Biçim Veri Araçlar Uzantılar Yardım

Location	Date	Time	T (°C)	RH (%)	P (hPa)	U_2 (m/s)	n (h)	Pe (mm)	ET_o (mm)	ETc (mm)	IWA1 (L)	IWA2 (L)	IWA3 (L)	ID1 (min)	ID2 (min)	ID3 (min)
Ipsala	16.05.2024	23:59:00	17	67	1001	2.55	11.25	0.00	4.32	3.57	342	513	684	17	26	34
Ipsala	17.05.2024	23:59:00	16	69	1003	3.48	11.46	0.00	4.85	04.02	385	578	770	19	29	38
Ipsala	18.05.2024	23:59:00	18	65	1002	3.67	11.82	0.00	5.26	4.37	455	683	910	23	35	46
Ipsala	19.05.2024	23:59:00	17	69	1006	4.26	11.92	0.00	3.68	03.05	318	477	636	16	24	32
Ipsala	20.05.2024	23:59:00	18	65	1005	3.85	11.96	0.00	5.43	4.51	470	705	940	24	36	48
Ipsala	21.05.2024	23:59:00	17	63	1006	4.18	11.97	0.00	4.54	3.77	361	542	722	18	27	36
Ipsala	22.05.2024	23:59:00	18	60	1008	3.62	11.97	0.00	3.81	3.16	303	454	606	15	23	30
Ipsala	23.05.2024	23:59:00	17	72	1006	3.34	11.92	0.00	4.61	3.82	366	549	732	18	27	36
Ipsala	24.05.2024	23:59:00	18	76	1004	3.58	11.87	0.00	5.24	4.34	416	624	832	21	31	42
Ipsala	25.05.2024	23:59:00	20	72	1007	4.12	11.85	0.00	4.38	3.63	348	522	696	17	26	34
Ipsala	26.05.2024	23:59:00	20	75	1006	3.45	11.25	0.00	3.84	3.18	305	457	610	15	23	30
Ipsala	27.05.2024	23:59:00	19	78	1002	3.28	11.32	0.00	3.67	03.05	291	437	582	15	23	30
Ipsala	28.05.2024	23:59:00	20	78	1008	3.25	11.68	0.00	3.55	2.95	282	423	564	14	21	28
Ipsala	29.05.2024	23:59:00	18	69	1004	3.87	11.77	0.00	4.34	3.60	344	516	688	17	26	34
Ipsala	30.05.2024	23:59:00	21	79	1005	4.26	11.82	0.00	5.28	4.38	419	629	838	21	32	42
Ipsala	31.05.2024	23:59:00	20	80	1003	3.82	11.87	0.00	5.18	4.30	411	617	822	21	32	42
Ipsala	01.06.2024	23:59:00	21	76	1005	3.86	12.08	0.00	5.74	4.76	456	684	912	23	35	46
Ipsala	02.06.2024	23:59:00	22	65	1007	3.56	12.15	0.00	5.86	4.86	465	698	930	23	35	46
Ipsala	03.06.2024	23:59:00	23	63	1004	4.24	12.33	0.00	6.12	05.08	486	729	972	25	38	50
Ipsala	04.06.2024	23:59:00	24	69	1002	4.43	12.36	0.00	6.24	5.18	495	743	990	25	38	50
Ipsala	05.06.2024	23:59:00	24	68	1005	3.78	12.38	0.00	6.21	5.15	493	740	986	25	38	50
Ipsala	06.06.2024	23:59:00	24	66	998	3.87	12.35	0.00	5.73	4.76	458	687	916	23	35	46
Ipsala	07.06.2024	23:59:00	25	63	1003	4.12	12.34	0.00	6.14	5.10	488	732	976	24	36	48
Ipsala	08.06.2024	23:59:00	25	62	1004	4.21	12.25	0.00	6.18	5.13	491	737	982	25	38	50
Ipsala	09.06.2024	23:59:00	24	63	1009	3.95	12.36	0.00	6.15	5.10	488	732	976	24	36	48
Ipsala	10.06.2024	23:59:00	25	59	1005	3.78	12.35	0.00	06.11	5.10	488	732	976	24	36	48
Ipsala	11.06.2024	23:59:00	25	62	1006	3.66	12.37	0.00	6.23	5.17	494	741	988	25	38	50
Ipsala	12.06.2024	23:59:00	25	64	1002	3.72	12.36	0.00	6.26	5.95	569	854	1138	28	42	56

Figure 6 - Cloud database

2.5. Reference evapotranspiration calculations

The foundation of this study is based on the Penman-Monteith Equation (1), which was modified by the FAO and is presented below (Allen et al. 1998). In the estimation of ET_0, it was assumed that the hypothetical reference crop corresponds to a well-watered, actively growing grass surface with a fixed height of 0.12 m, surface resistance of 70 s m^{-1}, and albedo of 0.23, as defined by FAO-56 guidelines. The parameters in the equation are derived from meteorological data that depends on both spatial and seasonal characteristics. Therefore, obtaining these data is the most critical step in calculating the ET_0. In the developed system, some of these parameters were obtained directly under field conditions using sensors, while others were retrieved via a mobile application based on location information (latitude) and daily average temperature. In this context, the sensor-based measurements include daily average temperature (T), daily average atmospheric pressure (P), average wind velocity at 2 meters height (U_2), daily sunshine duration (n), and daily average relative humidity (RH).

$$ET_0 = \frac{0.408 \times \Delta \times (R_n - G) + \gamma \times \frac{C_n}{(T+273)} \times U_2 \times (e_s - e_a)}{\Delta + \gamma \times (1 + C_d \times U_2)} \quad (1)$$

Where: ET_0 represents the reference evapotranspiration (mm day-1); Δ is the slope of the vapor pressure curve (kPa/°C); γ denotes the psychrometric constant (kPa/°C); R_n is the net radiation at the crop surface (MJ/m²/day); G is the soil heat flux density (MJ/m²/day), which is assumed to be zero; C_n is the numerator constant that depends on the reference crop type and the time step of the calculation (for a short crop and daily time step, C_n = 900); C_d is the denominator constant similarly based on

the reference crop and time step (C_d = 0.34 for a short crop and daily calculations); T is the mean daily air temperature at 2 meters height (°C); U_z is the average wind velocity measured at 2 meters height (m/s); e_s is the saturation vapor pressure at mean air temperature (kPa); and e_a is the actual vapor pressure at mean air temperature (kPa).

2.6. Evapotranspiration and irrigation water requirement

Equation 2 was used in the ET_C calculation. The daily average ET_0 values were adjusted using K_C coefficients to determine the daily average ET_C values. (Allen et al. 1998).

$$ET_C = ET_0 \times K_C \quad (2)$$

Where: ET_C: Rice evapotranspiration (mm), K_C: Crop coefficient. The Crop Water Consumption Guide for Irrigated Crops in Türkiye was used in the calculation of K_C (TAGEM 2017) (Table 3). The values of the K_C coefficients according to the growth stages were taken as the day after planting, and these values were used in the ET_C calculation with the software.

Table 3 - Seasonal crop coefficients

Stage (days)	*Crop Coefficient (K_C) Value*
Inıtial (0-27 days)	0.83
Mid (28-88 days)	1.19
Late (89- 135 days)	0.77

The amount of irrigation water (I) was determined by Eq. 3. As described in the Materials section, precipitation was measured using a pluviometer. Precipitation depth (mm) is measured with a tipping resolution of 0.2 mm, ensuring consistent and reliable performance under varying environmental conditions. Effective precipitation was assumed to be 80% of the total measured precipitation (TAGEM 2017; Kirchner 2024). The calculation of irrigation volume (V) was performed according to Equation 4. The water application efficiency was considered constant at 90% (Allen et al. 1998).

$$I = ET_C - Pe \quad (3)$$

Where: I represents the amount of irrigation water (mm), and Pe denotes the effective precipitation (mm).

$$V = I \times A \times Pw \quad (4)$$

Where: V is the irrigation volume (L), A is the area (m^2), and Pw is the wetted area fraction (taken as 1 since the entire area was irrigated).

Since the system was designed with a focus on automation, it was programmed to shut off automatically based on the irrigation duration. The irrigation duration was calculated using Equation 5 (Yıldırım, 2008). Operating pressure was kept constant during irrigation periods.

$$T = \frac{V}{Q} \times 60 \quad (5)$$

Where: T denotes the irrigation duration (minute), and Q represents the system flow rate per plot (L/h).

The system flow rate per plot was calculated using Equation 6 (Yıldırım, 2008).

$$Q = \frac{A}{(LD \text{ x } LE)} \text{ x } q \quad (6)$$

Where: LD represents the distance between laterals (m), LE is the spacing between emitters along the lateral (m), and q denotes the discharge rate of a single emitter (L/h).

The irrigation water use efficiency was calculated using Equation 7 based on the volume of irrigation water applied and yield parameters (Kresović et al. 2016; Wang et al. 2023).

$$IWUE = \frac{Y}{I} \quad (7)$$

Where: IWUE denotes the irrigation water use efficiency (kg/m^3); Y is the crop yield (kg/da); and I represents the volume of irrigation water applied (mm).

Economic water productivity (EWP) was estimated by relating the net economic income obtained from crop production to the total volume of irrigation water applied. Gross income was calculated as the product of yield and market price, and subsequently normalized by the amount of water used (Çetin & Kara 2019; Taş et al. 2021). In addition, a net return-based approach was considered by accounting for production costs in the economic assessment.

$$\mathrm{EWP} = \frac{\mathrm{NI}}{\mathrm{I}} \tag{8}$$

Where: EWP is water economic productivity ($/m^3), NI: net economic income per unit area ($/ha).

2.7. Statistical analysis

The differences among the data obtained from the study were evaluated using one-way analysis of variance (One-Way ANOVA) at a significance level of $p = 0.01$. When a significant difference was detected, Duncan's multiple comparison test was performed to identify which groups differed from one another. The lowercase letters presented in the tables indicate the distinctions among the groups. All statistical analyses were conducted using the SPSS 29.0 software.

3. Results and Discussion

3.1. Installation of the automation system and wetted area test

The experimental trials of the device were conducted at the Digital Agriculture Laboratory. The prototype was installed in the field after the completion of rice sowing in both growing seasons, s on June 13, 2023, and May 16, 2024, respectively (Figure 7). In the first year of the study, data collection continued until the final irrigation date of October 13, 2023, and in the second year until September 17, 2024. All data were stored in a Google Sheets database throughout both irrigation periods.

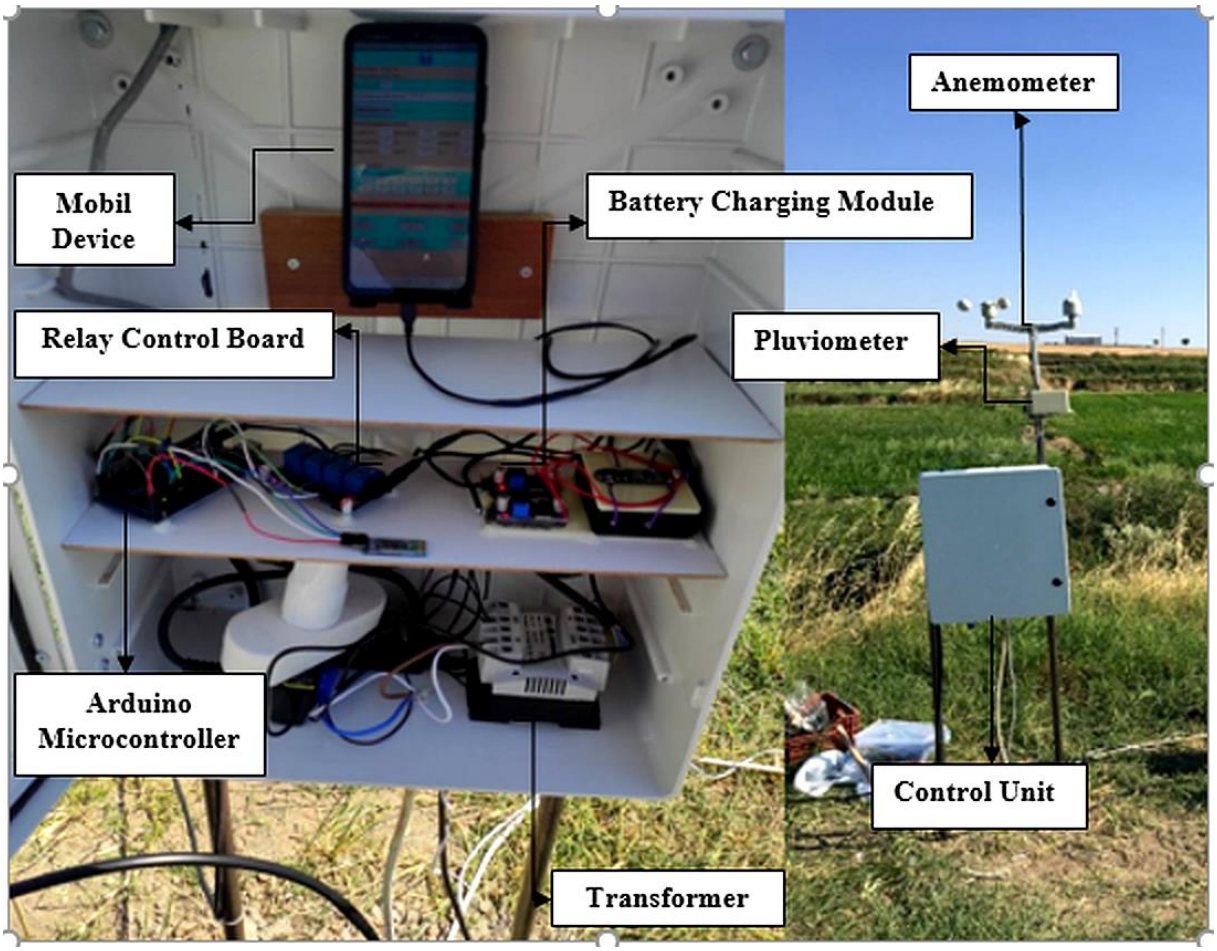


Figure 7 - Prototype device

Following the installation of the device, the plots within the experimental area were established. Prior to plot formation, a wetted volume test was conducted to determine whether the entire area could be adequately irrigated by the system. This test was

performed using 16 mm diameter laterals with a constant pressure of 1 atm and a flow rate of 4 L/h. The spacing between both emitters and laterals was set at 50 cm.

In the first year of the study, it was observed that the wetted area was fully covered within 20 minutes. On the previous day, the device recorded an ET_C value of 4.76 mm, and under these conditions, a total of 5.30 mm of irrigation water was applied. In the second year, full coverage of the wetted area was achieved within 15 minutes. On the first day the device was activated, the ET_C value was measured as 3.57 mm, and correspondingly, 3.97 mm of irrigation water was applied (Table 4).

Table 4 - Wetted area test results

2023		***2024***	
Time Period (min)	***Wetting Diameter (cm)***	***Time Period (min)***	***Wetting Diameter (cm)***
0-5	7	0-4	5
0-10	15	0-8	12
0-15	32	0-12	30
0-20	50	0-15	50

As a result of the wetted area test, it was determined that the device successfully performed irrigation automation. Pw of 1 was achieved during the test, in order to ensure proper field saturation and uniform emergence of the rice crop, irrigation was applied daily during the germination emergence period. In the first year of the study, 8.50 mm of irrigation water was applied per day, while in the second year, this amount was increased to 9 mm per day.

Analysis of the meteorological data recorded by the field installed device revealed that the average daily air temperature showed consistent trends in both 2023 and 2024, ranging between 14 °C and 29 °C in 2023, and between 16 °C and 30 °C in 2024. The seasonal average temperature was measured as 23 °C in the first year and 24 °C in the second year. Throughout the cultivation period in both seasons, daily average temperatures remained consistently above the base temperature threshold of 10 °C required for paddy rice growth (Peşkircioğlu et al. 2013; Kaya-Altop et al. 2022).

Relative humidity in the study area ranged from 50% to 79% in 2023 and from 44% to 82% in 2024, with corresponding seasonal averages of approximately 65% and 67%, respectively. Wind velocity followed a fluctuating pattern during the production periods in both years, varying between 2.58 m/s and 5.59 m/s in 2023, and between 1.96 m/s and 5.39 m/s in 2024. The average seasonal wind velocities were recorded as 4.11 m/s and 3.82 m/s for 2023 and 2024, respectively.

Seasonal atmospheric pressure values ranged from 996 hPa to 1015 hPa in 2023 and from 1001 hPa to 1020 hPa in 2024, with average pressures of 1005 hPa and 1009 hPa, respectively. In 2023, the sunshine duration was recorded as 12.41 hours, with minimum and maximum durations of 10.92 and 12.66 hours. In 2024, the sunshine duration was slightly lower at 12.01 hours, ranging from 10.52 to 12.46 hours. Total precipitation recorded at the study site was 14.65 mm in the first year and 19.56 mm in the second year (Figures 8 and 9).

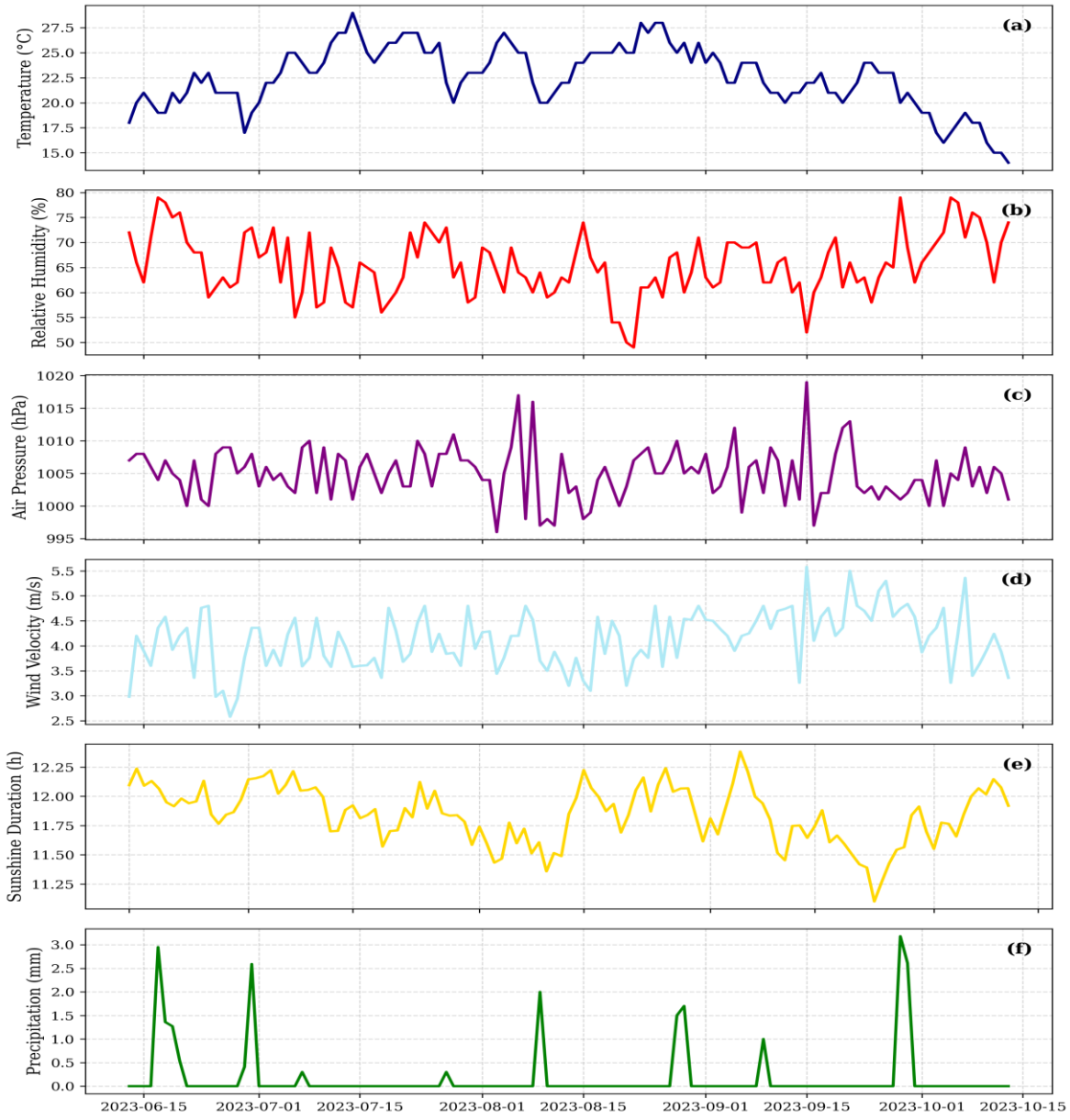


Figure 8 - Meteorological parameters during the 2023 growing season (13 June –13 October 2023). Subplots represent (a) average air temperature, (b) average relative humidity, (c) average air pressure, (d) average wind velocity, (e) sunshine duration, and (f) precipitation

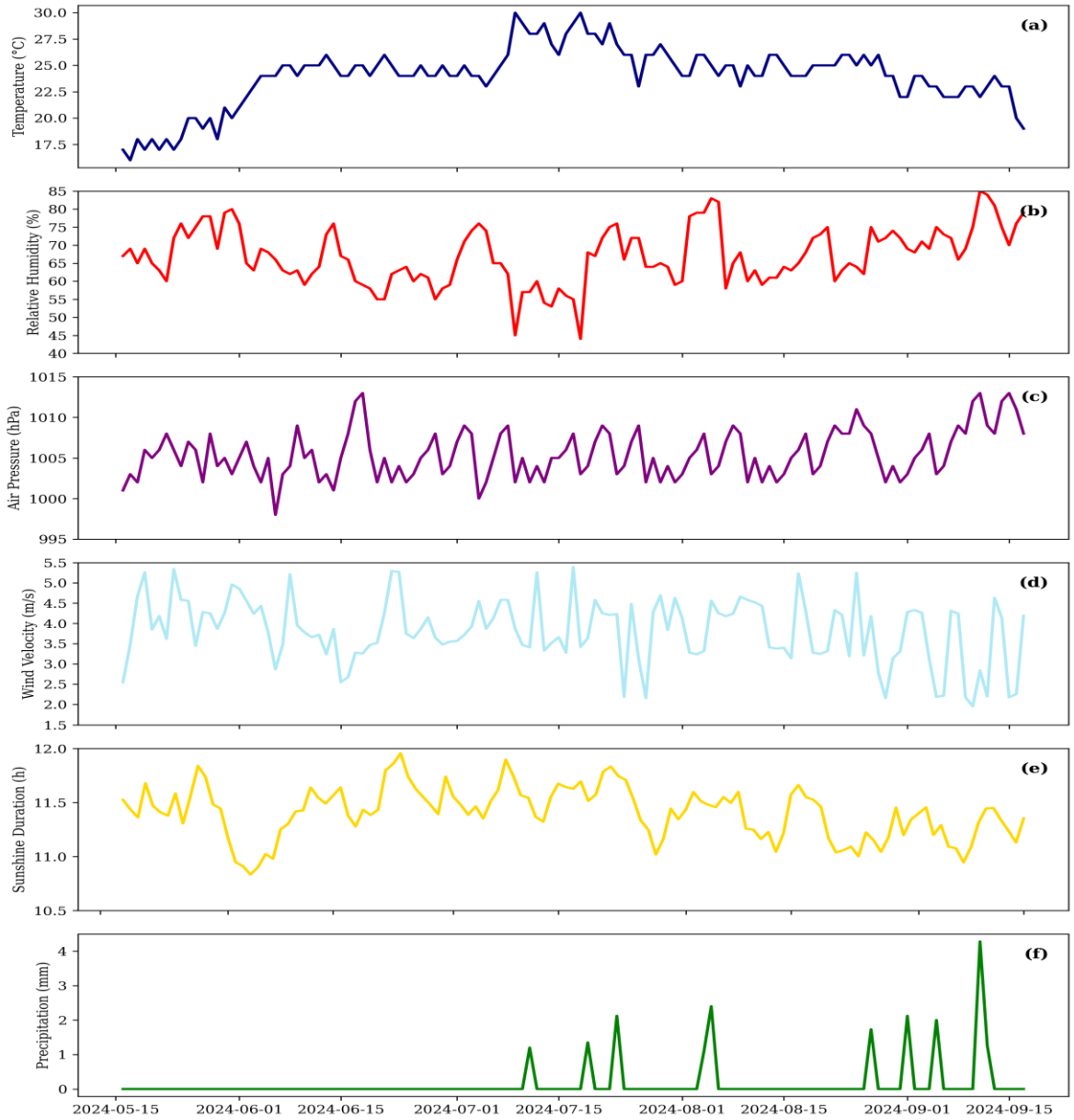


Figure 9 - Meteorological parameters during the 2024 growing season (16 May –17 September 2024). Subplots represent (a) average air temperature, (b) average relative humidity, (c) average air pressure, (d) average wind velocity, (e) sunshine duration, and (f) precipitation

3.2. Reference evapotranspiration and evapotranspiration values

In this study, a comparative analysis of daily ET_0 and ETc values was conducted for the growing seasons of 2023 and 2024, covering the period from May to September (Figure 10).

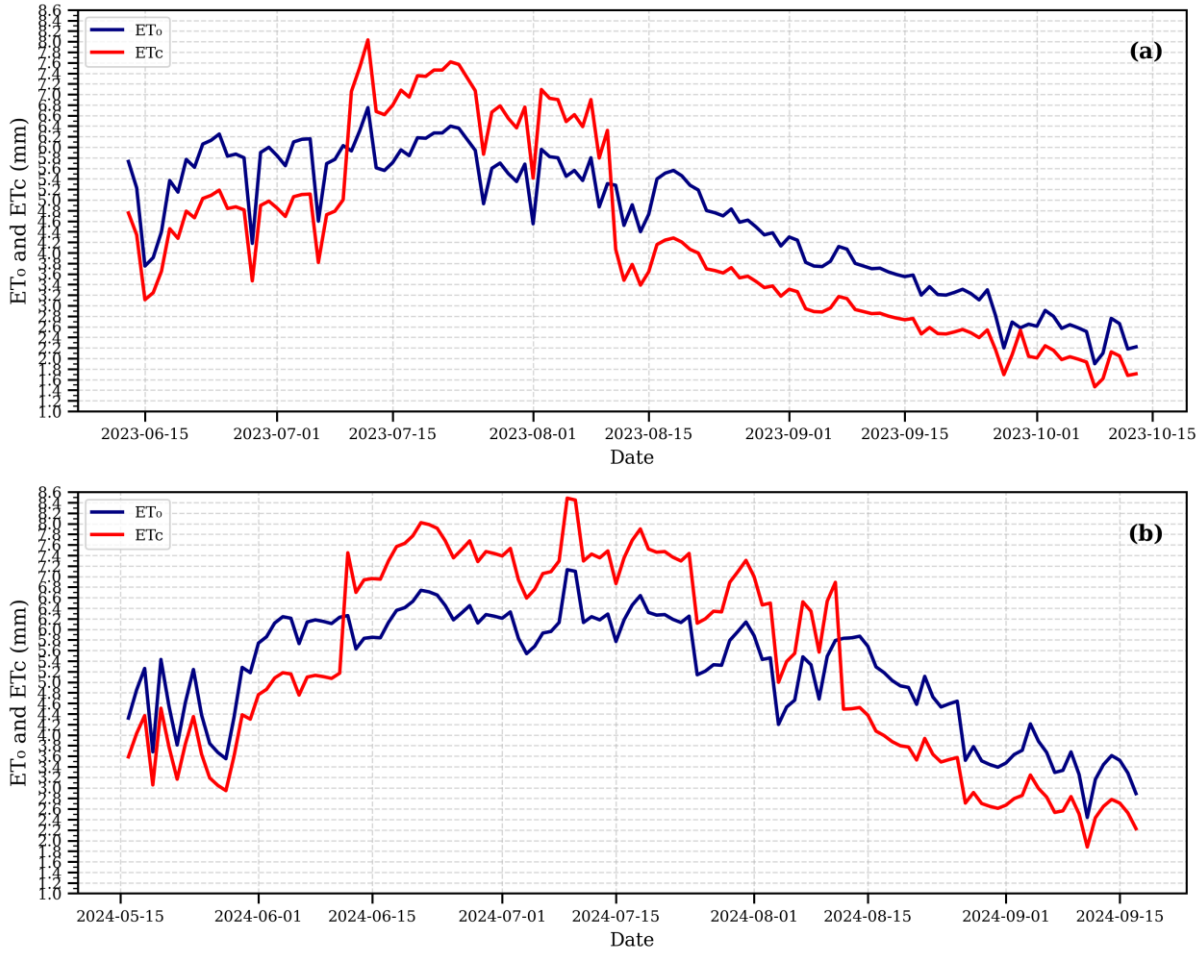


Figure 10 - ET_0 and ET_C during the growing seasons of 2023 (a) and 2024 (b).

Throughout the 2023 growing season, the total ET_0 and ETc values were measured as 571 mm and 583 mm, respectively, whereas in 2024, these values increased to 655 mm and 665 mm, respectively. In 2023, the maximum ET_0 and ET_C values were recorded on July 12, reaching 6.75 mm and 8.03 mm, respectively. Similarly, in 2024, the peak values occurred on July 9, with ET_0 reaching 7.13 mm and ET_C 8.48 mm. The timing of these peaks in early July for both years clearly reflects the impact of elevated summer temperatures and extended sunshine duration on atmospheric evaporative demand and plant water use. These high ET_0 and ETc levels correspond to the critical growth stages of the crop and serve as key indicators for determining optimal irrigation timing and volume. Conversely, the lowest ET_0 and ET_C values were observed in the late stages of the growing season, particularly in September. In 2023, minimum values of 1.90 mm for ET_0 and 1.47 mm for ET_C were recorded on October 8, 2023, whereas in 2024, the minimum values occurred on September 11, with ET_0 at 2.44 mm and ET_C at 1.88 mm. These decreases are attributed to seasonal changes such as declining air temperatures, increasing relative humidity, and the crop's transition into the harvest stage. The 2024 dataset exhibited consistently higher average values of both ET_0 and ET_C compared to 2023. This may suggest an increased atmospheric evaporative demand or enhanced crop activity during the 2024 season. Notably, from June 12 to July 21, 2024, ET_C values remained consistently above 7 mm, indicating a critical irrigation window characterized by intensive ET_C requirements. In contrast, a similar increase in 2023 was observed only for a shorter duration between late June and mid-July. The annual average ET_0 in 2023 was approximately 4.90 mm, while in 2024 it increased to around 5.30 mm. Similarly, the average ET_C rose from 4.00 mm in 2023 to about 4.90 mm in 2024. These interannual differences highlight the impact of climatic variability on crop water demand and emphasize the necessity for adaptive irrigation scheduling based on real time environmental conditions.

3.3. Irrigation water requirement and yield parameters

In both growing seasons of the study, irrigation practices were concluded ten days prior to harvest to facilitate field drying and harvesting operations. The rice harvest was conducted on October 23, 2023, in the first season, and on September 27, 2024, in the second season. At the early growth stage, from sowing until seedlings reached a height of approximately 10 cm, all treatments received uniform irrigation amounts defined as initial establishment irrigation. During this period, a total of 155 mm and 146 mm of irrigation water was applied across all treatments in 2023 and 2024, respectively (Table 5). These values were determined based on ET_C requirements to ensure rapid and uniform germination under the drip irrigation system. Throughout the active irrigation period, the developed prototype system automatically managed irrigation for the S100, S150, and S200 treatments

based on real time ET_C values calculated using the FAO-PM method. Table 5 presents the total seasonal irrigation water applied, the obtained grain yield, thousand grain weight and the corresponding IWUE values for each treatment.

Table 5 - Irrigation water and yield parameters

Season	*Treatment*	*Irrigation Amount (mm)*	*Grain yield (kg/ha)*	*IWUE (kg/m^3)*	*Thousand Grain Weight (g)*	*EWP ($\$/m^3$)*
2023	S100	695	4552 c	0.65	26.2 b	- 0.148
	S150	966	5474 bc	0.57	27.4 ab	- 0.024
	S200	1235	6403 ab	0.52	28.3 a	0.046
	F	1555	6502 a	0.42	28.8 a	0.042
2024	S100	802	5381 c	0.67	27.1 c	- 0.018
	S150	1156	6263 b	0.54	28.4 b	- 0.006
	S200	1492	7104 a	0.48	29.2 b	0.006
	F	1916	7401 a	0.39	30.3 a	0.018

Differences between means shown with different lowercase letters in the same row and column are significant and indicate the difference between levels (*P≤0.01 is significant, **P≥0.01 is not significant).

When examining the irrigation water amounts presented in Table 5, it is evident that the total seasonal irrigation water applied varied considerably among treatments. In the 2023 season, the total irrigation water applied ranged from 695 mm (S100) to 1555 mm (F), and in the 2024 season, from 802 (S100) mm to 1916 (F) mm. Across both years, the S100 treatment consistently received the least amount of irrigation water, while the F practise received the highest. A comparison of the total irrigation water applied under the F practice and other treatments reveals substantial differences. In 2023, the F applied 2.24, 1.78, and 1.39 times more irrigation water than S100, S150, and S200 treatments, respectively. Similarly, in 2024, the respective multipliers were 2.39, 1.86, and 1.44. This clearly demonstrates that prototype-controlled applications, particularly S100, are significantly more water efficient than F, using up to 55% and 58% less irrigation water in 2023 and 2024, respectively.

In both seasons, increasing irrigation water generally led to higher grain yield; however, the magnitude of yield gain diminished at higher water levels. In 2023, grain yield increased from 4552 kg/ha under S100 to 5474 kg/ha and 6403 kg/ha under S150 and S200 treatments, respectively. F achieved the highest yield (6502 kg/ha), but it was not statistically different from S200, indicating that near maximum yield could be obtained without applying excessive irrigation water. A similar trend was observed in 2024, where grain yield ranged from 5381 kg/ha (S100) to 7104 kg/ha (S200), while the F treatment produced the highest yield (7401 kg/ha).

Despite higher yields under increased irrigation, IWUE consistently declined as irrigation water amount increased. In 2023, IWUE decreased from 0.65 kg/m³ in S100 to 0.42 kg/m³ in the F treatment. Likewise, in 2024, the highest IWUE was recorded in S100 (0.67 kg/m³), whereas the lowest was observed under full irrigation (0.39 kg/m³). These results indicate that deficit irrigation treatments, particularly S100 and S150, enhanced water productivity by producing relatively high yields with substantially lower water inputs.

Thousand grain weight (TGW) responded positively to increased irrigation levels in both seasons. In 2023, TGW increased from 26.2 g under S100 to 28.8 g under F, while in 2024 it increased from 27.1 (S100) g to 30.3 g (F). The statistically significant differences among treatments suggest that improved grain filling under higher soil moisture conditions contributed to yield increases. However, the relatively small differences in TGW between S200 and F treatments further support the conclusion that excessive irrigation provides limited additional benefits in terms of yield components. Seasonal comparisons revealed that grain yield and TGW were generally higher in 2024 than in 2023, likely due to more favorable climatic conditions and improved crop adaptation to drip irrigation management. Nevertheless, the overall response pattern to irrigation levels remained consistent across years, highlighting the robustness of the observed trends.

EWP values demonstrated substantial variability among irrigation treatments and between the two growing seasons, highlighting the dynamic interaction between water use, crop yield, and economic conditions. In 2023, EWP values ranged from 0.148 to 0.046 $\$/m^3$, with S100 and S150 resulting in negative values, indicating that the generated income was insufficient to cover production costs. In contrast, both S200 and F treatments produced positive EWP values, with S200 exhibiting the highest economic efficiency. This result suggests that moderate deficit irrigation enabled a more effective allocation of water resources by maintaining relatively high yields while reducing water input.

A markedly different pattern was observed in 2024. Although negative EWP values persisted under lower irrigation levels (S100 and S150), all treatments showed improved economic performance compared to 2023. F achieved the highest EWP value (0.018 $\$/m^3$), surpassing S200, which exhibited a considerably lower value (0.006 $\$/m^3$). This shift indicates that the additional water applied under full irrigation was economically justified in 2024, as the resulting yield increase outweighed both the higher water use and elevated production costs.

The inter-annual variation in EWP clearly demonstrates that economic efficiency of irrigation water is not solely governed by agronomic responses but is also strongly influenced by external economic factors, including input costs, crop prices, and exchange rates. Despite higher water consumption, full irrigation became more advantageous in 2024 due to improved yield response and favorable economic conditions relative to water use. Conversely, in 2023, the marginal benefit of additional irrigation water diminished, making S200 the most economically efficient treatment.

Overall, these findings emphasize that the optimal irrigation strategy from an economic perspective is not constant but varies across seasons. The results underline the importance of integrating economic indicators such as EWP into irrigation management decisions, particularly under conditions of increasing water scarcity and fluctuating market conditions.

From an economic standpoint, the yield improvements associated with increasing irrigation levels should be evaluated in terms of marginal gains rather than absolute production. Although F resulted in the highest yield values, this increase was accompanied by a clear decline in IWUE, indicating that additional water inputs contribute progressively less to yield formation. This response reflects the principle of diminishing marginal productivity, where further increases in input result in relatively smaller yield increments. Similar relationships between irrigation level, yield, and water productivity have been highlighted in recent studies (Nigatu et al. 2024; Awa et al. 2025). When water costs, energy consumption, and operational expenses are considered, the economic justification of excessive irrigation becomes increasingly uncertain.

Within this context, the S150 and S200 treatments provide a more balanced alternative by maintaining relatively high yield levels while reducing total water input and improving IWUE compared to F. These treatments enhance water productivity and increase the potential economic return per unit of water applied. This is particularly relevant in semi-arid and water-limited environments, where irrigation management should aim not only to maximize yield but also to optimize economic performance and sustainability.

Therefore, although F may maximize yield under ideal conditions, S150 and S200 emerge as more economically viable and sustainable approaches under practical constraints. By maintaining yield within acceptable limits while reducing water and energy consumption, these strategies (S150 and S200) support both farm-level profitability and the long-term sustainability of water resources.

3.4. System cost

The total cost of the system, including the mini weather station, sensors, and other auxiliary electronic components, was determined to be approximately 215 USD $ based on January 2026 prices (Table 6). As can be seen, a very low cost system was designed for an automation system with these features. The methods and technologies used were found to be more economical compared to imported systems. Unlike conventional systems where unit costs vary depending on the irrigated area size, the unit costs of the current system do not change. Due to the operating principle of the system, the meteorological station and its associated control unit (Arduino Mega development board, voltage converter circuit, wireless communication device, relay triggering unit) can theoretically be used to irrigate areas of unlimited size. Since the control unit only triggers relays to open and close solenoid valves, it is capable of controlling solenoid valves of different diameters and quantities. Therefore, making a cost calculation based on the irrigated area size would not provide realistic data.

Table 6 - System cost parameters

Component	*Specification / Function*	*Unit Price ($)*
Arduino Mega 2560 R3 Development Board	Central control and data processing unit	16
Voltage Converter Module (Buck/Boost)	Power regulation and compatibility	4
Wireless Communication Module	Long range communication with mobile/remote interface	13
Relay Module (4-channel)	Switching control for solenoid valves	8
Mini weather station	Includes temperature, humidity, air pressure, light and wind sensors	85
Solenoid Valves (4 pcs)	12V DC, 1-inch, drip line-compatible (control units)	26
Waterproof Enclosure and Mounting Materials	Field protection and weather resistance	8
Wiring, Connectors, Power Supply (Misc.)	Auxiliary electronics and power adapters	5
Drip Irrigation Line and Fittings	main polyethylene pipeline, lateral drip lines, start connectors, end caps, tees, elbows, couplers, filter unit and pressure regulator	40
Total		215 USD $

To further emphasize the cost-effectiveness and technical advantages of the developed system, a comparative evaluation with similar irrigation automation systems reported in the literature is presented in Table 7. This comparison highlights differences in

system architecture, data acquisition methods, automation levels, clearly demonstrating the novelty and practicality of the proposed approach.

Table 7 - Smart irrigation system comparison

Reference	*Methodology*	*Data Source*	*Description*
Osroosh et al. 2016	A wireless control and monitoring system	Air temperature, solar radiation, relative humidity, wind speed, and rainfall	When cost efficiency and system simplicity are prioritized, the climate-based irrigation automation approach was found to provide an adequate water supply while effectively preventing crop water stress.
Barkunan et al. 2019	Smartphone-based soil moisture estimation system	Air temperature, relative humidity, light and rainfall	Smart sensor-based irrigation system achieved significant water savings (41.43% and 13.03% relative to flood and drip irrigation, respectively), while improving irrigation efficiency and reducing labor requirements, thereby demonstrating strong potential for scalable and data-driven agricultural water management applications.
Zia et al. 2021	IoT-based irrigation optimization	Soil moisture, air temperature and relative humidity	The findings revealed that the IoT-enabled irrigation system significantly enhanced irrigation efficiency, achieving substantial water savings and yield improvement compared to conventional practices under field conditions.
S et al. 2023	IoT sensor-based threshold drip irrigation	Soil moisture, air temperature, relative humidity and soil temperature	Threshold controlled drip irrigation system outperformed ETC-based scheduling by enhancing plant growth parameters, reducing irrigation duration, and achieving considerable water savings under controlled conditions.
Kushwaha et al. 2024	Integrated IoT-based adaptive irrigation monitoring framework	Soil moisture and soil temperature	System effectively enhanced real-time soil monitoring accuracy and energy efficiency, leading to more reliable and optimized irrigation management under field conditions.
Singh et al. 2025	IoT-enabled low cost weighing lysimeter development	Soil moisture, soil temperature and ultrasonic sensor	IoT-enabled digital weighing lysimeter provides highly accurate, real-time evapotranspiration measurements with minimal operational cost, offering a scalable and efficient tool for advanced irrigation management and water-use optimization.

In contrast to the predominantly soil moisture driven or hybrid sensing approaches reported in Table 7, the proposed system estimates ET_0 directly from low cost meteorological measurements and autonomously determines irrigation requirements without relying on soil sensors. By leveraging the FAO Penman–Monteith equation with simplified, readily accessible climatic inputs, the system enables continuous and reliable estimation of crop water demand while minimizing hardware complexity. This design choice substantially enhances field applicability, particularly in large-scale agricultural areas, where the deployment, calibration, and maintenance of dense soil sensor networks often pose significant logistical and economic constraints.

Furthermore, eliminating soil-based sensing components reduces issues associated with spatial variability, sensor drift, and frequent recalibration, which are commonly reported limitations in sensor-dependent irrigation systems. Unlike lysimeter-based approaches that provide high accuracy but remain costly and impractical for widespread adoption, the proposed framework offers a balanced solution by combining acceptable accuracy with affordability and operational simplicity. The integration of real-time data acquisition, automated decision-making, and user-friendly control interfaces further supports efficient irrigation scheduling while reducing labor requirements and human intervention.

In addition, the system's reliance on meteorological data facilitates seamless integration with existing weather stations and online data sources, thereby enabling remote accessibility and scalability across different agro-climatic regions without substantial infrastructure modifications. This adaptability is particularly advantageous under conditions of increasing water scarcity and climate variability, where dynamic and responsive irrigation strategies are essential for sustainable crop production.

4. Conclusions

The findings of this study demonstrate that the developed irrigation automation system, based on the FAO Penman–Monteith model and integrated with a low cost mini weather station, effectively calculated real time evapotranspiration and automatically managed drip irrigation for paddy rice under field conditions. The prototype successfully maintained system stability throughout both growing seasons and ensured precise water application according to the calculated crop water requirements.

When the irrigation levels were compared, significant differences in irrigation water use and yield performance were observed between treatments. F applied 2.2–2.4 times more irrigation water than the S100 treatment, yet achieved similar yields. Despite receiving up to 51% less water, the S100 treatment provided statistically comparable grain yield to F and achieved the highest IWUE (0.65–0.67 kg/m^3). This result confirms that irrigation scheduling strictly based on real time ET_C not only reduces water consumption but also maintains crop productivity and quality.

The S200 treatment, which represented double the ET_C-based irrigation, resulted in only a marginal yield increase compared to the F, while consuming nearly the same or slightly less water. Therefore, the S200 and F treatments exhibited diminishing water productivity, emphasizing that excessive irrigation does not necessarily improve yield but increases water loss and production costs.

Overall, the system reduced irrigation water requirements without compromising yield or grain quality, showing that automation and climate-based irrigation control can provide up to 50% water savings under paddy conditions. The modular, low cost design (≈215 USD) and mobile-based user interface make the system particularly suitable for small and medium sized rice farms. Moreover, its open source hardware and software structure allow easy adaptation for different crops and climatic regions.

The results indicate that the developed system represents a cost effective and sustainable alternative to conventional paddy irrigation, aligning with the objectives of climate smart agriculture. Future research should focus on integrating soil moisture sensors and cloud based analytics for predictive irrigation management, enabling even greater precision and resilience under variable climatic conditions.

Author Declarations

Authors' contributions: Visualization: H.F.A., Data Curation: H.F.A., Formal Analysis: H.F.A., Resources: H.F.A., Literature Search: H.F.A., Ü.A., Field Work: H.F.A., H.N., Writing: H.F.A., Ü.A., G.Ç., Methodology: H.F.A., Ü.A., G.Ç., S.A., H.N., Conceptualization: H.F.A., Ü.A., G.Ç., S.A., H.N., Software: H.F.A., Ü.A., S.A., Editing: Ü.A., G.Ç., Project Administration: Ü.A., Funding Acquisition: Ü.A.

Conflict of interest/Competing interests: The authors declare no conflict of interest.

Ethics approval/declarations: No need/ Not applicable.

Funding: The authors declare that the study was supported by Scientific and Technological Research Council of Türkiye (Grant Numbers: 122O082)

Consent to participate: No need/ Not applicable.

Acknowledgements

We would like to thank İlkay GÖZE and Hasan GÖZE for their assistance during the fieldwork.

References

Aksu S & Kızıl Ü (2020). Design and testing of flexibility sensors to be used in agricultural engineering applications. *COMU Journal of Agriculture Faculty* 8(2): 271-276. https://doi.org/10.33202/comuagri.726746

Allen R G, Pereira L S, Raes D & Smith M (1998). Crop evapotranspiration. Guidelines for computing crop water requirements. *FAO Irrig. Drain*. Paper No. 56, Rome.

Amin M M, Akter A, Jahangir M R & Ahmed T (2021). Leaching and runoff potential of nutrient and water losses in rice field as affected by alternate wetting and drying irrigation. *Journal of Environmental Management* 297, 113402. https://doi.org/10.1016/j.jenvman.2021.113402

Awa M, Yusuying A, Zhao J & Tumaerbai H (2025). Impact of drip irrigation levels on the growth, production, and water productivity of quinoa grown in arid climate conditions. *Water* 17(7): 917. https://doi.org/10.3390/w17070917

Barkunan S R, Bhanumathi V & Sethuram J (2019). Smart sensor for automatic drip irrigation system for paddy cultivation. *Computers and Electrical Engineering* 73, 180-193. https://doi.org/10.1016/j.compeleceng.2018.11.013

Cai J, Liu Y, Lei T & Pereira L S (2007). Estimating reference evapotranspiration with the FAO Penman-Monteith equation using daily weather forecast messages. *Agricultural and Forest Meteorology* 145(2007):22-35

Celestin S, Qi F, Li R, Yu T & Cheng W (2020). Evaluation of 32 simple equations against the penman–monteith method to estimate the reference evapotranspiration in the Hexi Corridor, northwest China. *Water* 12(10): 2772. https://doi.org/10.3390/w12102772

Córdova M, Carrillo-Rojas G, Crespo P, Wilcox B & Célleri R (2015). Evaluation of the Penman-Monteith (FAO 56 PM) method for calculating reference evapotranspiration using limited data. *Mountain Research and Development* 35(3): 230-239. https://doi.org/10.1659/MRD-JOURNAL-D-14-0024.1

Çetin O & Kara A (2019). Assesment of water productivity using different drip irrigation systems for cotton. *Agricultural Water Management, 223*, 105693. https://doi.org/10.1016/j.agwat.2019.105693

Çığ F, Erden Z & Toprak Ç C (2024). Registered paddy (oryza sativa l.) varieties in Türkiye, paddy agriculture potential and recent developments in paddy agriculture. *International Journal of Food, Agriculture and Animal Sciences* 4 (1): 55-62

Dai A, Zhao T & Chen J (2018). Climate change and drought: a precipitation and evaporation perspective. *Current Climate Change Reports* 4: 301-312. https://doi.org/10.1007/s40641-018-0101-6

Dai L, Fu R, Zhao Z, Guo X, Du Y, Hu Z & Cao G (2022). Comparison of fourteen reference evapotranspiration models with lysimeter measurements at a site in the humid Alpine Meadow, northeastern Qinghai-Tibetan Plateau. *Frontiers in Plant Science* (13): 854196. doi: 10.3389/fpls.2022.854196.

Darko A M, Danquah E O, Dormatey R, Keteku A K, Frimpong F, Adjah K L, Osei-Wusu M O, Ayamba B E, Ofosu K A, Dankwa K O & Danquah F O (2025). Global rice production: current status, challenges, and future scenarios. *Rice Cultivation Under Abiotic Stress*, 3-21. https://doi.org/10.1016/B978-0-443-21793-7.00001-5

Demirel K, Çamoğlu G, Tatar O, Nar H, Boran A, Eroğlu I & Genç L (2020). Use of subsurface drip irrigation and water retention barrier to effective use of water in rice. *Mustafa Kemal University Journal of Agricultural Sciences* 25(2): 108-121. https://doi.org/10.37908/mkutbd.678748

Er-Raki S, Chehbouni A, Guemouria N, Duchemin B, Ezzahar J & Hadria R (2007). Combining FAO-56 model and ground-based remote sensing to estimate water consumptions of wheat crops in a semi-arid region. *Agricultural Water Management* 87(1): 41-54. https://doi.org/10.1016/j.agwat.2006.02.004

Gaytancıoğlu O & Yılmaz F (2024). Sustainable paddy farming in edirne: evaluating the impacts of excessive fertilizer and pesticide use. *Sustainability* 16(17): 7814. https://doi.org/10.3390/su16177814

Glauber J W & Mamun A (2024). Global rice market: Current outlook and future prospects. IFPRI Discussion Paper 2310. Washington, DC: International Food Policy Research Institute. Available from: https://hdl.handle.net/10568/168523

Gündoğdu K S, Traore F, Kouadio L & Hessels T (2020). Estimating in-season actual evapotranspiration over a large-scale irrigation scheme in resource-limited conditions. *Proceedings of the Bulgarian Academy of Sciences* 73(10): 1473-1480. https://doi.org/10.7546/CRABS.2020.10.18

Hashim N, Ali M M, Mahadi M R, Abdullah A F, Wayayok A, Kassim M S M & Jamaluddin A (2024). Smart farming for sustainable rice production: an insight into application, challenge, and future prospect. *Rice Science*, 31(1): 47-61. https://doi.org/10.1016/j.rsci.2023.08.004

Irmak S, Irmak A, Allen R G & Jones J W (2003). Solar and net radiation-based equations to estimate reference evapotranspiration in humid climates. *Journal of Irrigation and Drainage Engineering* 29(5): 336-347

Islam S & Alam A R (2021). Performance evaluation of FAO Penman-Monteith and best alternative models for estimating reference evapotranspiration in Bangladesh. *Heliyon* 7(7). https://doi.org/10.1016/j.heliyon.2021.e07487

Kaya-Altop E, Uysal M S, Haghnama K & Mennan H (2022). Environmental factors on seasonal germination of different weedy rice (oryza sativa l.) biotypes. *Ciência Rural* 53(2), e20210728. https://doi.org/10.1590/0103-8478cr20210728

Kondaveeti H K, Kumaravelu N K, Vanambathina S D, Mathe S E & Vappangi S (2021). A systematic literature review on prototyping with Arduino: Applications, 94 challenges, advantages, and limitations. *Computer Science Review* 40, 100364. https://doi.org/10.1016/j.cosrev.2021.100364

Kızıl Ü, Aksu S, Kınacı A C, Bilgücü E & Şentürklü S (2022). A sound-based monitoring and evaluation system for small-scale dairy operations. *Journal of Advanced Research in Natural and Applied Sciences* 8(3): 380-390. https://doi.org/10.28979/jarnas.1081753

Köksal E S, Tunca E & Taner S Ç (2022). Irrigation management by using digital technologies. *Water and Wastewater Management: Global Problems and Measures*, 247-267. https://doi.org/10.1007/978-3-030-95288-4_20

Kresović B, Tapanarova A, Tomić Z, Životić L, Vujović D, Sredojević Z & Gajić B (2016). Grain yield and water use efficiency of maize as influenced by different irrigation regimes through sprinkler irrigation under temperate climate. *Agricultural Water Management* 169: 34-43. https://doi.org/10.1016/j.agwat.2016.01.023

Kulmány I M, Bede-Fazekas Á, Beslin A, Giczi Z, Milics G, Kovács B, Kovács M, Bálint A, Bede L & Vona V (2022). Calibration of an Arduino-based low-cost capacitive soil moisture sensor for smart agriculture. *Journal of Hydrology and Hydromechanics* 70(3): 330-340. https://doi.org/10.2478/johh-2022-0014

Kushwaha Y K, Joshi A, Panigrahi R K & Pandey A (2024). Development of a smart irrigation monitoring system employing the wireless sensor network for agricultural water management. *Journal of Hydroinformatics* 26(12): 3224-3243. https://doi.org/10.2166/hydro.2024.241

Lang D, Zheng J, Shi J, Liao F, Ma X, Wang W, Chen X & Zhang M A (2017). Comparative study of potential evapotranspiration estimation by eight methods with FAO Penman-Monteith method in southwestern China. *Water* 9(10): 734. https://doi.org/10.3390/w9100734

Li X, Chen D, Cao X, Luo Z & Webber M (2020). Assessing the components of, and factors influencing, paddy rice water footprint in China. *Agricultural Water Management* 229: 105939. http://doi.org/10.1016/j.agwat.2019.105939

Moratiel R, Bravo R, Saa A, Tarquis A M & Almorox J (2020). Estimation of evapotranspiration by the Food and Agricultural Organization of the United Nations (FAO) Penman-Monteith temperature (PMT) and Hargreaves-Samani (HS) models under temporal and spatial criteria-a case study in Duero basin (Spain). *Natural Hazards and Earth System Sciences* 20(3): 859-875. https://doi.org/10.5194/nhess-20-859-2020

Nabipour R, Yazdani M R, Mirzaei F, Ebrahimian H & Mobaraki F A (2024). Water productivity and yield characteristics of transplanted rice in puddled soil under drip tape irrigation. *Agricultural Water Management* 295: 108753. https://doi.org/10.1016/j.agwat.2024.108753

Nigatu B, Getu D, Getachew T & Getaneh B (2024). Effect of irrigation regime on yield component and water use efficiency of tomato at Ataye irrigation scheme, Ataye Ethiopia. *Italian Journal of Agrometeorology* (2): 89–100. https://doi.org/10.36253/ijam-2492

Ogidan O K, Oluwagbayide S D & Ale T (2023). A microcontroller-based irrigation scheduling using FAO Penman-Monteith equation. *Turkish Journal of Agricultural Engineering Research* 4(1): 15-25. https://doi.org/10.46592/turkager.1170630

Osroosh Y, Peters R T, Campbell C S & Zhang Q (2016). Comparison of irrigation automation algorithms for drip-irrigated apple trees. *Computers and Electronics in Agriculture* 128, 87-99. https://doi.org/10.1016/j.compag.2016.08.013

Parthasarathi T, Vanitha K, Mohandass S & Vered E (2018). Evaluation of drip irrigation system for water productivity and yield of rice. *Agronomy Journal* 110(6): 2378-2389. https://doi.org/10.2134/agronj2018.01.0002

Pearce R H, Chadwick M A & Francis R (2024). Experiential learning in physical geography using Arduino low-cost environmental sensors. *Journal of Geography in Higher Education* 48(1): 54-73. https://doi.org/10.1080/03098265.2022.2155804

Peşkircioğlu M, Torunlar H, Alsancak S B, Özaydın K A, Mermer A, Şahin M, Tuğaç M G, Aydoğmuş O, Emeklier Y, Yıldırım Y E & Kodal S (2013). Determination of potential rice (oryza sativa l.) cultivation areas of Turkey using geographic ınformation system techniques. *Journal of Field Crops Central Research Institute* 22(1): 20-25

Qiu J, Shen Z & Xie H (2023). Drought impacts on hydrology and water quality under climate change. *Science of the Total Environment* 858(1): 159854. https://doi.org/10.1016/j.scitotenv.2022.159854

S V K, Singh C D, Rao K V, Kumar M & Rajwade Y A (2023). Development of a smart IoT-based drip irrigation system for precision farming. *Irrigation & Drainage*, 72(1). https://doi.org/10.1002/ird.2757

Samoy-Pascual K, Lampayan R M, Remocal A T, Orge R F, Tokida T & Mizoguchi M (2022). Optimizing the lateral dripline spacing of drip-irrigated aerobic rice to increase water productivity and profitability under the water-limited condition. *Field Crops Research* 287: 108669. https://doi.org/10.1016/j.fcr.2022.108669

Sentelhas P C, Gillespie T J & Santos E A (2010). Evaluation of FAO Penman-Monteith and alternative methods for estimating reference evapotranspiration with missing data in Southern Ontario, Canada. *Agricultural Water Management* 97(5): 635-644. https://doi.org/10.1016/j.agwat.2009.12.001

Sharda R, Mahajan G, Siag M, Singh A & Chauhan B S (2017). Performance of drip-irrigated dry-seeded rice (oryza sativa l.) in South Asia. Paddy and Water Environment, 15(1): 93-100. https://doi.org/10.1007/s10333-016-0531-5

Singh, R K, Gupta A & Kumar M (2025). Advancing precision irrigation through an affordable IoT-enabled lysimeter for monitoring crop water requirements. Frontiers in Sustainable Food Systems, 9, 1677654. https://doi.org/10.3389/fsufs.2025.1677654

Surendran U, Raja P, Jayakumar M & Subramoniam S R (2021). Use of efficient water saving techniques for production of rice in India under climate change scenario: A critical review. *Journal of Cleaner Production* 309: 127272. https://doi.org/10.1016/j.jclepro.2021.127272

TAGEM (2017). Republic of Türkiye Ministry of Agriculture and Forestry General Directorate Of Agricultural Research And Policies. Available from: https://www.tarimorman.gov.tr/TAGEM/Belgeler/yayin/Türkiyede%20Sulanan%20Bitkilerin%20Bitki%20Su%20Tüketimleri.pdf

Taş İ, Coşkun Y, Akçura M, Kaplan M & Gökalp Z (2021). Economic analysis of paddy production with drip irrigation: case study of Dardanelles-Turkey. *Current Trends in Natural Sciences* 11(21): 455-473. https://doi.org/10.47068/ctns.2022.v11i21.050

Tunca E & Köksal E S (2024). Evaluating the impact of different UAV thermal sensors on evapotranspiration estimation. *Infrared Physics & Technology* 136: 105093. doi: https://doi.org/10.1016/j.infrared.2023.105093

Tüzüner A (1990). Handbook of soil and water analysis laboratories. Ministry of Agriculture and Rural Affairs, General Directorate of Rural Services Publication, 374 pp., Ankara. (In Turkish). TÜİK (2025) Turkish Statistical Institute, Available from: https://data.tuik.gov.tr/Kategori/GetKategori?p=tarim-111

Wang X, Tian W, Zheng W, Shah S, Li J, Wang X & Zhang X (2023). Quantitative relationships between salty water irrigation and tomato yield, quality, and irrigation water use efficiency: A meta-analysis. *Agricultural Water Management* 280: 108213. https://doi.org/10.1016/j.agwat.2023.108213

Yazdanpanah M, Zobeidi T, Sieber S, Löhr K & Homayoon S B (2022). Replacing rice with lower water consumption crops. *Climate Research* 88: 101-114. https://doi.org/10.3354/cr01700

Yıldırım O (2008). Design of irrigation systems. *Ankara University Faculty of Agriculture Publication*, No. 1565, Textbook No. 518, Ankara, 353 pp. (In Turkish)..

Yıldırım M, Yücel M & Mucan U (2025). Solar-powered automated drip irrigation system scheduling. *Journal of Agricultural Sciences* 31(4): 1012-1023. https://doi.org/10.15832/ankutbd.1598746

Zia H, Rehman A, Harris N R, Fatima S & Khurram M (2021). An experimental comparison of IoT-based and traditional irrigation scheduling on a flood-irrigated subtropical lemon farm. *Sensors* 21(12), 4175. https://doi.org/10.3390/s21124175

Copyright 2026 The Author(s). This is an open-access article published by Faculty of Agriculture, Ankara University under the terms of the Creative Commons Attribution License which permits unrestricted use, distribution, and reproduction in any medium or format, provided the original work is properly cited.